Formation Tracking With Size Scaling of Double Integrator Agents

Djati Wibowo Djamari[1,✉], Asif Awaludin[2], Halimurrahman Halimurrahman[2], Rommy Hartono[3], Patria Rachman Hakim[3], Adi Wirawan[4], Haikal Satrya Utama[1], Tiara Kusuma Dewi[1]

[1]Mechanical Engineering Study Program, Sampoerna University, Indonesia
[2]Research Center for Climate and Atmosphere, National Research and Innovation Agency, Indonesia
[3]Research Center for Satellite Technology, National Research and Innovation Agency, Indonesia
[4]Research Center for Aeronautics Technology, National Research and Innovation Agency, Indonesia
djati.wibowo@sampoernauniversity.ac.id✉

Abstract

This paper considers the problem of distributed formation scaling of Multi-Agent Systems (MASs) under a switching-directed graph where the scaling of formation is determined by one leader agent. A directed-sensing graph where neighboring agents exchange their relative displacement and a directed-communication graph where neighboring agents exchange the information about formation scaling factor and velocity factors are used in this paper. One leader agent which decides the formation scaling factor as well as the velocity of the group is chosen among agents. It is shown that under a switching-directed graph, the group of agents achieves the desired formation pattern with the desired scaling factor as well as the desired group's velocity if the union of the sensing and communication graphs contains a directed spanning tree.

Keywords: *Scalable Formation, Double Integrator, Switching Network, Formation Tracking.*

Received: 06 December 2023
Accepted: 09 February 2024
Online: 18 February 2024
Published: 30 June 2024

1 Introduction

Study on cooperative control of MASs has received a lot of attention from the research community in the last decade due to MAS potential applications in satellite [6], [18], [9], spacecraft [21], [17], unmanned aerial vehicle (UAV) [22], [1], [14], and many more. One of the well-known problems in the MAS is formation control and it has been studied by many, see [7], [16], [13], [8], [20], [2], [5], to mention a few. The basic method in formation control is to add a bias in the consensus algorithm, and this bias contains the formation pattern.

When using the standard formulation of the relative displacement-based formation control problem (see for example [16]), it is assumed that the entire agent knows the desired formation parameters (formation pattern and size). Additionally, the produced formation pattern is static and we can only modify the formation parameters (i.e. size and pattern of formation) by keying in different desired formation parameters to each agent. If the formation size needs to be changed during the operation, it will lead to an inefficient operation if the standard formulation of displacement-based formation control is used because the entire agent must be recalled to the central station so that the new formation parameters can be keyed into all of the agents.

A recent study by Djamari in [5] discusses formation control with size scaling. That is, the size of the formation can be adjusted during the operation of MAS. The method in [5] is based on self-loop Laplacian and distributed observer where the size of the formation depends on the initial states and graph topology. Formation with size scaling capability does make sense when the group of agents must change their formation size due to changes in mission objectives or environmental changes. An example of the application of formation control with size scaling is satellite-based measurement calibration using a multi-drone system.

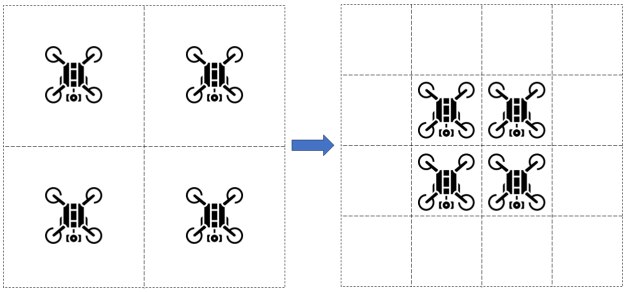

Figure 1: Drone formation change their size to achieve different resolution.

A satellite, for example, can be used to measure the ground temperature, and this measurement has a certain resolution. The calibration can be done by using a thermal camera mounted on a drone (UAV), and the drone is programmed to fly below the satellite during the measurement calibration. The use of a single drone for satellite-based measurement calibration can be found in the work of [12]. However, when using a single drone, the calibration can only cover a small por-

tion of the area since the coverage area of the thermal camera is limited. A multi-drone system can be deployed to calibrate the whole satellite's measurement area coverage. Moreover, the resolution of the drone's measurement can be adjusted by changing the drone's formation size as shown in Figure 1. The left picture in Figure 1 shows a coarse resolution measurement while the right picture in Figure 1 shows a finer resolution measurement. Note that the formation shape/pattern of the group does not change (it remains a rectangular formation).

The early works of formation control with size scaling can be found in [3], [2], and [19]. The work of [3] considered the distributed formation scaling problem of double integrator agents under an undirected-unweighted and fixed sensing graph, while the communication graph uses a directed and fixed graph. The work of [3] used the incidence matrix entries in the distributed control algorithm. Thus, the algorithm can only be applied if the sensing graph is undirected-unweighted. Furthermore, the state chosen in the work is the relative displacement between neighboring agents. This makes the algorithm not suitable for switching graph analysis. The work of [3] was extended by [19] by exchanging more variables to adjust the rotational angle of the formation and its translation. Although the flexibility of the formation is improved, and also connectivity maintenance was also discussed in the work, the work of [19] was still using undirected-unweighted and fixed graphs for all communication and sensing graphs.

In the work of [2], the desired scaling factor is known only by the leader agents, and it is estimated by the follower. The estimation algorithm is based on the ratio between the true and the desired relative displacements of neighboring agents. The work of [2] uses the small-gain theorem to show that the distributed scalable formation is achievable. While the algorithm does not use the communication network to distribute the desired scaling factor, the desired scalable formation is only achievable under certain graph conditions. And thus, the connectivity of the sensing graph alone is not sufficient in achieving the desired scalable formation.

The proposed algorithms in [2], [3], [19], and [5] work only for fixed graph settings. Recent work by [4] proposes scalable formation under switching graph topology, and the algorithm is based on the internal model principle. However, the internal model principle algorithm is prone to system's instability due to model mismatch. In this work, we propose a distributed scalable formation algorithm for double integrator agents, and we consider switching directed graph topology (for both sensing and communication graphs). The contributions of this work are the following:

- Extension of the works [3] and [2] to switching directed graph topology.
- Producing a result (see *Theorem 2*) which shows that certain dynamics with switching state matrix can be converted into consensus dynamics with switching graph topology. These results also show that the algorithm in the previous work [4] can achieve formation under directed switching graph topology.

The notation used in this paper is standard. Non-negative and positive integer sets are indicated by $\mathbb{Z}_0^+$ and $\mathbb{Z}^+$ respectively. Let $m, \ell \in \mathbb{Z}^+$ with $m > \ell$. Then $\mathbb{Z}^m := \{1, 2, \cdots, m\}$ and $\mathbb{Z}_\ell^m := \{\ell, \ell+1, \cdots, m\}$. While $\mathbb{R}, \mathbb{R}^+, \mathbb{R}^n, \mathbb{R}^{n\times m}$ refer respectively to the sets of real numbers, the sets of positive real numbers, n-dimensional real vectors and n by m real matrices. I_n is the $n \times n$ identity matrix with 1_n being the n-column vector of all ones (subscript omitted when the dimension is clear). The transpose of matrix M and vector v are indicated by M' and v' respectively. Additional notations are introduced when required in the text.

2 Preliminaries

2.1 Graph Notations

A directed graph G is defined by a pair of finite set of nodes ($V = \{v_1, ..., v_N\}$) and a set of edges ($E \subseteq V \times V$), thus $G = (V, E)$. An edge is represented by an ordered pair of nodes, i.e. $e_q = (v_i, v_j) \in E$. This way, node v_i is called the parent node, while node v_j is called the child node. This also means that information is flowing from node v_i to node v_j (or v_i is a neighbor to v_j). Let $\hat{G}$ be the subgraph of G, then $\hat{G}$ can be defined as the following: $\hat{G} = (\hat{V}, \hat{E})$ where $\hat{V} \subseteq V$ and $\hat{E} \subseteq E$.

A path from node v_i to node v_j is an ordered edge in the form $(v_{i_p}, v_{i_{p+1}})$ where $p = 1, ..., q-1$. A directed spanning tree is a directed graph where there is one node called the root which has no parent node, and there is a directed path from the root node to every other node. A directed graph G is said to contain a directed spanning tree if graph G has a directed spanning tree as its subgraph.

The adjacency matrix, $\mathbb{A} = [a_{ij}] \in \mathbf{R}^{NxN}$ is associated with the graph G, where if $(v_j, v_i) \in E$ then $a_{ij} > 0$ and $a_{ij} = 0$ otherwise. Note that a_{ij} is the weight of the edge $(v_j, v_i) \in E$. By default, $a_{ii} = 0$ unless stated otherwise in this paper. The case where $a_{ii} > 0$ is when the graph has a self-loop. The *Laplacian* matrix, $L = [l_{ij}] \in \mathbf{R}^{NxN}$ is defined as $l_{ii} = \sum_{j\neq i} a_{ij}$ and $l_{ij} = -a_{ij}; i \neq j$.

Following are standard results on spectral properties of the *Laplacian* matrix and consensus analysis of single integrator model MAS that we will use in this paper:

Lemma 1. [[15], Lemma 3.3] Let L be the *Laplacian* matrix associated with directed graph G. Zero is an eigenvalue of L with $1_N = [1, ..., 1]^T \in \mathbf{R}^N$ as the corresponding right eigenvector, and all of the nonzero eigenvalues of L have positive real parts. Furthermore, zero is a simple eigenvalue of L if and only if G contains a directed spanning tree.

Lemma 2. [[10], Theorem 3.12] Let L be the *Laplacian* matrix associated with directed graph G. Let $y^T L = 0$, $Lq = 0$ and $q^T y = 1$. The system $\dot{p}(t) = -Lp(t)$ has trajectories that satisfy: $\lim_{t\to\infty} p(t) = (y^T p(t_0))q$ for any $p(t_0)$ if and only if the directed graph G contains directed spanning tree.

Remark 1. By default, $t_0 = 0$ in this paper, unless stated otherwise.

2.2 Problem Statement

We consider N double integrator agents' model with the position of agent i denoted as $x_i \in \mathbf{R}$ and its velocity denoted as $v_i \in \mathbf{R}$ as the following:

$$\begin{aligned} \dot{x}_i &= v_i \\ \dot{v}_i &= u_i \end{aligned} \quad i = 1, ..., N \tag{1}$$

where $u_i \in \mathbf{R}$ is the control signal of agent i. Let $\boldsymbol{x}^d = [x_1^d, ..., x_N^d]^T \in \mathbf{R}^N$ be the vector of the desired formation pattern which is known by all of the agents, $\lambda^* \in \mathbf{R}$ be the desired scaling factor of the formation and $\gamma^* \in \mathbf{R}$ be the desired velocity of the group. Both λ^* and γ^* are constants and known only by the leader agent, where we assume that there is one leader agent in the group. The following are the objectives defined in this paper:

$$\lim_{t\to\infty} v_i(t) = \gamma^* \tag{2}$$

$$\lim_{t\to\infty} (x_i(t) - x_j(t)) = \lambda^* \left(x_i^d - x_j^d\right) \tag{3}$$

We can see that $x_i(t)$ that satisfies $\lim_{t\to\infty} x_i(t) = c + x_i^* = c + \lambda^* x_i^d + \gamma^* t \quad \forall i$ also satisfies the objective (3). This means that the scaled formation pattern of the group is preserved in spite of the constant bias c. The constant bias c is determined by the initial value of agents' positions and velocities which will be shown later. The formation tracking lies in objective (2), where all agents are required to track the same velocity.

Our method is to exchange the variable λ and γ between neighboring agents aside from exchanging the position states. The interaction to exchange the position states is labeled as the *sensing graph* while the interaction to exchange the variables λ and γ is labeled as the *communication graph*.

3 Formation and Velocity Scaling under Fixed Sensing and Communication Topologies

In this section, we assume that the sensing and communication graphs are both fixed. We also assume that each agent is able to measure its own velocity and it can measure its relative displacement with its neighbors. We propose the following distributed control law:

$$\begin{aligned} u_i(t) = &- \sum_{j\in\mathcal{N}_i} a_{ij}[(x_i(t) - x_j(t)) - \lambda_i(t)(x_i^d - x_j^d)] \\ &- k(v_i(t) - \gamma_i(t)) \end{aligned} \tag{4}$$

$$\dot{\lambda}_i(t) = - \sum_{j\in\bar{\mathcal{N}}_i} \alpha_{ij}(\lambda_i(t) - \lambda_j(t)) \tag{5}$$

$$\dot{\gamma}_i(t) = - \sum_{j\in\bar{\mathcal{N}}_i} \alpha_{ij}(\gamma_i(t) - \gamma_j(t)) \tag{6}$$

where $\mathcal{N}_i$ and $\bar{\mathcal{N}}_i$ denote the neighborhood of agent i in the sensing graph G and communication graph F respectively, a_{ij} is the entry of the i^{th} row and j^{th} column of the adjacency matrix associated with the sensing graph G, α_{ij} is the entry of the i^{th} row and j^{th} column of the adjacency matrix associated with the communication graph F, $k > 0$ is a tuned-scalar parameter. Meanwhile, $\lambda_i \in \mathbf{R}$ and $\gamma_i \in \mathbf{R}$ are numbers stored in agent i, for all $i \in \mathbb{Z}^N$, which correspond to the formation scaling factor and velocity factor, and they are updated using (5) and (6). Note that both G and F are directed graphs.

Without loss of generality, agent N is chosen as the leader agent that knows and determine the formation scaling and velocity factors. Therefore, in (5) and (6), we set $\alpha_{Nj} = 0; \forall j$. It also follows that $\lambda_N(t) = \lambda^*$ and $\gamma_N(t) = \gamma^*$ for all $t \geq 0$.

Let $\boldsymbol{x} = [x_1, \cdots, x_N]^T$, $\boldsymbol{v} = [v_1, \cdots, v_N]^T$, $\boldsymbol{\lambda} = [\lambda_1, \cdots, \lambda_N]^T$, and $\boldsymbol{\gamma} = [\gamma_1, \cdots, \gamma_N]^T$. The agents' dynamics can be written in matrix form as the following:

$$\begin{bmatrix} \dot{\boldsymbol{x}}(t) \\ \dot{\boldsymbol{v}}(t) \\ \dot{\boldsymbol{\lambda}}(t) \\ \dot{\boldsymbol{\gamma}}(t) \end{bmatrix} = \begin{bmatrix} \mathbf{0} & \mathbf{I} & \mathbf{0} & \mathbf{0} \\ -L & -k\mathbf{I} & \Gamma & k\mathbf{I} \\ \mathbf{0} & \mathbf{0} & -H & \mathbf{0} \\ \mathbf{0} & \mathbf{0} & \mathbf{0} & -H \end{bmatrix} \begin{bmatrix} \boldsymbol{x}(t) \\ \boldsymbol{v}(t) \\ \boldsymbol{\lambda}(t) \\ \boldsymbol{\gamma}(t) \end{bmatrix} \tag{7}$$

where $\mathbf{0}$ and $\mathbf{I}$ are matrix of all zeros and identity matrix with appropriate dimension, respectively. $L \in \mathbf{R}^{NxN}$ and $H \in \mathbf{R}^{NxN}$ are the corresponding *Laplacian* matrices associated with sensing graph G and communication graph F, respectively. $\Gamma = diag\{\sum_{j=1}^N l_{1j}x_j^d, \ldots, \sum_{j=1}^N l_{Nj}x_j^d\} \in \mathbf{R}^{NxN}$, where l_{ij} is the entry of i^{th} row and j^{th} column of L, $i = 1, \ldots, N$.

Define position error and its derivative:

$$\begin{aligned} \tilde{\boldsymbol{x}}(t) &= \boldsymbol{x}(t) - \boldsymbol{x}^* = \boldsymbol{x}(t) - (\boldsymbol{\lambda}^* \boldsymbol{x}^d + \boldsymbol{\gamma}^* 1_N t) \\ \dot{\tilde{\boldsymbol{x}}}(t) &= \dot{\boldsymbol{x}}(t) - \boldsymbol{\gamma}^* 1_N = \boldsymbol{v}(t) - \boldsymbol{\gamma}^* 1_N \end{aligned} \tag{8}$$

Define velocity error and its derivative:

$$\begin{aligned} \tilde{\boldsymbol{v}}(t) &= \boldsymbol{v}(t) - \boldsymbol{\gamma}^* 1_N = \dot{\tilde{\boldsymbol{x}}}(t) \\ \dot{\tilde{\boldsymbol{v}}}(t) &= \dot{\boldsymbol{v}}(t) \end{aligned} \tag{9}$$

Define formation scaling error and its derivative:

$$\begin{aligned} \tilde{\boldsymbol{\lambda}}(t) &= \boldsymbol{\lambda}(t) - \boldsymbol{\lambda}^* 1_N \\ \dot{\tilde{\boldsymbol{\lambda}}}(t) &= \dot{\boldsymbol{\lambda}}(t) \end{aligned} \tag{10}$$

Define velocity factor error and its derivative:

$$\begin{aligned} \tilde{\boldsymbol{\gamma}}(t) &= \boldsymbol{\gamma}(t) - \boldsymbol{\gamma}^* 1_N \\ \dot{\tilde{\boldsymbol{\gamma}}}(t) &= \dot{\boldsymbol{\gamma}}(t) \end{aligned} \tag{11}$$

By noting that $L\boldsymbol{x}^d = \Gamma 1_N$ and $L1_N = H1_N = 0_N$, the error dynamics can be written as the following:

$$\begin{bmatrix} \dot{\tilde{\boldsymbol{x}}}(t) \\ \dot{\tilde{\boldsymbol{v}}}(t) \\ \dot{\tilde{\boldsymbol{\lambda}}}(t) \\ \dot{\tilde{\boldsymbol{\gamma}}}(t) \end{bmatrix} = \begin{bmatrix} \mathbf{0} & \mathbf{I} & \mathbf{0} & \mathbf{0} \\ -L & -k\mathbf{I} & \Gamma & k\mathbf{I} \\ \mathbf{0} & \mathbf{0} & -H & \mathbf{0} \\ \mathbf{0} & \mathbf{0} & \mathbf{0} & -H \end{bmatrix} \begin{bmatrix} \tilde{\boldsymbol{x}}(t) \\ \tilde{\boldsymbol{v}}(t) \\ \tilde{\boldsymbol{\lambda}}(t) \\ \tilde{\boldsymbol{\gamma}}(t) \end{bmatrix} \tag{12}$$

From (12), it can be seen that the error dynamics of the formation scaling and velocity factors are independent from the error dynamics of the velocity and position. We can therefore analyze the convergence of the error dynamics of the formation scaling and velocity factors separately from the position and velocity errors dynamics.

3.1 Convergence of Error Dynamics $\tilde{\lambda}$ and $\tilde{\gamma}$

Based on (12), the dynamics of $\tilde{\lambda}$ and $\tilde{\gamma}$ are

$$\dot{\tilde{\boldsymbol{\lambda}}}(t) = -H\tilde{\boldsymbol{\lambda}}(t),$$

and

$$\dot{\tilde{\boldsymbol{\gamma}}}(t) = -H\tilde{\boldsymbol{\gamma}}(t).$$

The following *Theorem* provides the condition for the convergence of states $\tilde{\lambda}$ and $\tilde{\gamma}$.

Lemma 3. Suppose the graph F contains directed spanning tree, the states $\tilde{\lambda}$ and $\tilde{\gamma}$ converge to zero exponentially $\forall \tilde{\lambda}_i(0), \tilde{\gamma}_i(0) \in \mathbf{R}; i = 1, \ldots, N-1$.

Proof. Note that $\tilde{\lambda}_N(t) = \tilde{\gamma}_N(t) = 0$ for all $t \geq 0$ since $\lambda_N(t) = \lambda^*$ and $\gamma_N(t) = \gamma^*$ for all $t \geq 0$. Since the graph F contains directed spanning tree, referring to the work of [11], the dynamics of $\tilde{\lambda}$ and $\tilde{\gamma}$ reach consensus exponentially. Moreover, the speed of convergence is determined by the first nonzero eigenvalue of H. On the other hand, due to $\tilde{\lambda}_N(t) = \tilde{\gamma}_N(t) = 0$ for all $t \geq 0$, then all states of $\tilde{\lambda}$ and $\tilde{\gamma}$ approach zero exponentially. □

3.2 Convergence of Error Dynamics $\tilde{x}$ and $\tilde{v}$

Based on *Lemma 3*, assuming that the graph F contains directed spanning tree, the states $\tilde{\boldsymbol{\lambda}}$ and $\tilde{\boldsymbol{\gamma}}$ converge to zero exponentially, and the dynamics of (12) can be reduced to:

$$\begin{bmatrix} \dot{\tilde{\boldsymbol{x}}}(t) \\ \dot{\tilde{\boldsymbol{v}}}(t) \end{bmatrix} = \begin{bmatrix} \mathbf{0} & \mathbf{I} \\ -L & -k\mathbf{I} \end{bmatrix} \begin{bmatrix} \tilde{\boldsymbol{x}}(t) \\ \tilde{\boldsymbol{v}}(t) \end{bmatrix} = [\Omega] \begin{bmatrix} \tilde{\boldsymbol{x}}(t) \\ \tilde{\boldsymbol{v}}(t) \end{bmatrix}; t > t_0 \tag{13}$$

To analyze the convergence of $\tilde{\boldsymbol{x}}$ and $\tilde{\boldsymbol{v}}$, we will start with the following *Lemma*:

Lemma 4. Let $\beta_i \in spec(\Omega)$, $\mu_i \in spec(-L)$, G be the graph associated with L and $spec(\cdot)$ is the set of the eigenvalue of $(\cdot)$. Ω has at least one zero eigenvalue with the corresponding eigenvector of $[1_N^T, 0_N^T]^T$. Let k be chosen such that

$$k > \max_{i, \mu_i \neq 0} \sqrt{\frac{(\mathrm{Im}\,(\mu_i))^2}{|\mathrm{Re}\,(\mu_i)|}}.$$

Then, the zero eigenvalue of Ω is simple if and only if graph G contains directed spanning tree, and the nonzero eigenvalues of Ω have negative real parts.

Proof. The eigenvalues of Ω are the solution to the following:

$$|\beta \mathbf{I}_{2N} - \Omega| = \begin{vmatrix} \beta\mathbf{I} & -\mathbf{I} \\ L & (\beta + k)\mathbf{I} \end{vmatrix} = 0$$

where $I_{2N} \in \mathbf{R}^{2Nx2N}$ is the identity matrix, $|(\cdot)|$ denotes the determinant of $(\cdot)$. It is a well-known fact that:

$$\begin{vmatrix} A & B \\ C & D \end{vmatrix} = |A||D - CA^{-1}B| = |AD - ACA^{-1}B|$$

The eigenvalue problem of Ω can therefore be written as:

$$|(\beta(\beta + k))\mathbf{I} - \beta \mathbf{I} L \frac{1}{\beta}\mathbf{I}(-\mathbf{I})| = |(\beta(\beta + k))\mathbf{I} + L| = 0$$

Since $\mu_i \in spec(-L)$, it implies that $\beta_i(\beta_i + k) = \mu_i$ or

$$\beta_i \pm = \frac{1}{2}\left(-k \pm \sqrt{k^2 + 4\mu_i}\right). \tag{14}$$

From the spectral properties of Laplacian matrix, we note that $-L$ has at least one zero eigenvalue and its nonzero eigenvalues lie in the open left half plane. Next, we will discuss the value of β_i for several cases of μ_i.

Case when $\boldsymbol{\mu_i = 0}$

Inserting $\mu_i = 0$ into (14) we obtain

$$\begin{aligned} \beta_i \pm &= \frac{1}{2}\left(-k \pm \sqrt{k^2 + 4 \cdot 0}\right) \\ &= \frac{1}{2}\left(-k \pm k\right) \\ \beta_i \pm &= 0, -k. \end{aligned}$$

Therefore, $\mu_i = 0$ corresponds to one $\beta_i = 0$ and one $\beta_i = -k$.

Case when $\boldsymbol{\mu_i < 0, \mu_i \in \mathbb{R}}$

Inserting μ_i into (14) we obtain

$$\beta_i \pm = \frac{1}{2}\left(-k \pm \sqrt{k^2 + 4\mu_i}\right)$$

Since $\mu_i < 0$, the following is always true

$$k > \mathrm{Re}\left(\sqrt{k^2 + 4\mu_i}\right).$$

Thus, $\mathrm{Re}\,(\beta_i) < 0$ holds for all $\mu_i \neq 0$. We can also conclude that when $\mu_i \in \mathbb{R}$, $k > 0$ is sufficient to make nonzero eigenvalues of Ω to be on the left-half plane.

Case when $\boldsymbol{\mu_i \in \mathbb{C}, \mathrm{Re}\,(\mu_i) < 0}$

Let $\mu_i = \mathrm{Re}\,(\mu_i) + \mathrm{Im}\,(\mu_i)\,j$, we then write (14) as follows:

$$\begin{aligned} \beta_i \pm &= \frac{1}{2}\left(-k \pm \sqrt{k^2 + 4\left(\mathrm{Re}\,(\mu_i) + \mathrm{Im}\,(\mu_i)\right)}\right) \\ &= \frac{1}{2}\left(-k \pm \sqrt{(k^2 + 4\mathrm{Re}\,(\mu_i)) + 4\mathrm{Im}\,(\mu_i)\,j}\right) \end{aligned}$$

to analyze the square root of the complex part above, we write:

$$\sqrt{(k^2+4\mathrm{Re}\,(\mu_i))+4\mathrm{Im}\,(\mu_i)\,j}=c_i+d_ij$$

where c_i and d_i are the real part and imaginary part of $\sqrt{(k^2+4\mathrm{Re}\,(\mu_i))+4\mathrm{Im}\,(\mu_i)\,j}$, respectively. We want to show that for some choice of k, $k>c_i$ for all μ_i which would results in $\mathrm{Re}\,(\beta_i)<0$ for all $\mu_i\neq 0$. Then, we perform the following analysis:

$$\left(\sqrt{(k^2+4\mathrm{Re}\,(\mu_i))+4\mathrm{Im}\,(\mu_i)\,j}\right)^2=(c_i+d_ij)^2$$
$$\left(k^2+4\mathrm{Re}\,(\mu_i)\right)+4\mathrm{Im}\,(\mu_i)\,j=c_i^2+2c_id_ij-d_i^2$$

Equating the real and imaginary terms we obtain:

$$k^2+4\mathrm{Re}\,(\mu_i)=c_i^2-d_i^2 \tag{15a}$$
$$4\mathrm{Im}\,(\mu_i)=2c_id_i \tag{15b}$$

From (15b), $d_i=\frac{2\mathrm{Im}(\mu_i)}{c_i}$. Substitute d_i into (15a) we obtain:

$$k^2+4\mathrm{Re}\,(\mu_i)-c_i^2+\left(\frac{2\mathrm{Im}\,(\mu_i)}{c_i}\right)^2=0$$

Then, multiply both sides with c_i^2 and rearranging we get

$$c_i^4-c_i^2\left(k^2+4\mathrm{Re}\,(\mu_i)\right)-4\left(\mathrm{Im}\,(\mu_i)\right)^2=0$$

where c_i^2 is obtained from

$$c_{i,\pm}^2=\frac{\left(k^2+4\mathrm{Re}\,(\mu_i)\right)\pm\sqrt{\left(k^2+4\mathrm{Re}\,(\mu_i)\right)^2+16\left(\mathrm{Im}\,(\mu_i)\right)^2}}{2}$$

Since we need $k>c_i$ and we only concern with the positive and real values of c_i, we force the following relation:

$$k>c_i$$
$$k^2>c_i^2$$
$$k^2>\frac{\left(k^2+4\mathrm{Re}\,(\mu_i)\right)\pm\sqrt{\left(k^2+4\mathrm{Re}\,(\mu_i)\right)^2+16\left(\mathrm{Im}\,(\mu_i)\right)^2}}{2}$$

rearranging we obtain:

$$k^2-4\mathrm{Re}\,(\mu_i)>\pm\sqrt{\left(k^2+4\mathrm{Re}\,(\mu_i)\right)^2+16\left(\mathrm{Im}\,(\mu_i)\right)^2}$$

then, squaring both sides we get:

$$\left(k^2-4\mathrm{Re}\,(\mu_i)\right)^2>\left(k^2+4\mathrm{Re}\,(\mu_i)\right)^2+16\left(\mathrm{Im}\,(\mu_i)\right)^2$$
$$-16k^2\mathrm{Re}\,(\mu_i)>16\left(\mathrm{Im}\,(\mu_i)\right)^2$$

By noting that $\mathrm{Re}\,(\mu_i)<0$ for $\mu_i\neq 0$, we have

$$16k^2\left|\mathrm{Re}\,(\mu_i)\right|>16\left(\mathrm{Im}\,(\mu_i)\right)^2$$
$$k>\sqrt{\frac{\left(\mathrm{Im}\,(\mu_i)\right)^2}{\left|\mathrm{Re}\,(\mu_i)\right|}}$$

Finally, to guarantee $k>c_i$ for all i, we write

$$k>\max_{i,\mu_i\neq 0}\sqrt{\frac{\left(\mathrm{Im}\,(\mu_i)\right)^2}{\left|\mathrm{Re}\,(\mu_i)\right|}}.$$

Next, we discuss the possibility of algebraic and geometric multiplicity of μ_i. Suppose that $\mu_i\in spec(-L)$ has algebraic multiplicity of r with geometric multiplicity of one. We then have $-L\mathbf{v}_1=\mu_i\mathbf{v}_1;\ldots;-L\mathbf{v}_r=\mu_i\mathbf{v}_r$. Therefore for the first eigenvector of Ω we have:

$$\Omega\begin{bmatrix}w_1^a\\w_1^b\end{bmatrix}=\begin{bmatrix}\mathbf{0}&\mathbf{I}\\-L&-k\mathbf{I}\end{bmatrix}\begin{bmatrix}w_1^a\\w_1^b\end{bmatrix}=\beta_i\begin{bmatrix}w_1^a\\w_1^b\end{bmatrix}$$

From the first row we have $w_1^b=\beta_iw_1^a$ while from the second row we have $-Lw_1^a-kw_1^b=\beta_iw_1^b$. By subsituting the first row to the second row and analogously apply it for the rest of the eigenvectors we can have the following:

$$\Omega\begin{bmatrix}\mathbf{v}_1\\\beta_i\mathbf{v}_1\end{bmatrix}=\beta_i\begin{bmatrix}\mathbf{v}_1\\\beta_i\mathbf{v}_1\end{bmatrix};\ldots;\Omega\begin{bmatrix}\mathbf{v}_r\\\beta_i\mathbf{v}_r\end{bmatrix}=\beta_i\begin{bmatrix}\mathbf{v}_r\\\beta_i\mathbf{v}_r\end{bmatrix}$$

This part shows that for $\mu_i\in spec(-L)$ with algebraic multiplicity of r, each $\beta_i\in spec(\Omega)$ that satisfy $\beta_i(\beta_i+k)=\mu_i$ also has algebraic multiplicity of r. This part also shows that when $\beta_i=0$, the corresponding eigenvector is $[1_N^T,0_N^T]^T$ by noting that $\mathbf{v}=1_N$ where $-L\mathbf{v}=0$.

Suppose that $\mu_i\in spec(-L)$ has geometric multiplicity of $\bar{r}$. We then have $(\mu_iI+L)\mathbf{v}_1=0;(\mu_iI+L)\mathbf{v}_2=\mathbf{v}_1;\ldots;(\mu_iI+L)\mathbf{v}_{\bar{r}}=\mathbf{v}_{\bar{r}-1}$. By some algebraic manipulation we can have for Ω as the following:

$$(\beta_iI_{2N}-\Omega)\begin{bmatrix}\mathbf{v}_1\\\beta_i\mathbf{v}_1\end{bmatrix}=0;$$
$$(\beta_iI_{2N}-\Omega)\begin{bmatrix}\theta\mathbf{v}_2\\\beta_i\theta\mathbf{v}_2-\mathbf{v}_1\end{bmatrix}=\begin{bmatrix}\mathbf{v}_1\\\beta_i\mathbf{v}_1\end{bmatrix};\ldots;$$
$$(\beta_iI_{2N}-\Omega)\begin{bmatrix}\theta^{\bar{r}-1}\mathbf{v}_{\bar{r}}\\\beta_i\theta^{\bar{r}-1}\mathbf{v}_{\bar{r}}-\theta^{\bar{r}-2}\mathbf{v}_{\bar{r}-1}\end{bmatrix}$$
$$=\begin{bmatrix}\theta^{\bar{r}-2}\mathbf{v}_{\bar{r}-1}\\\beta_i\theta^{\bar{r}-2}\mathbf{v}_{\bar{r}-1}-\theta^{\bar{r}-3}\mathbf{v}_{\bar{r}-2}\end{bmatrix}$$

where $\theta=2\beta_i+k$. This part shows that for $\mu_i\in spec(-L)$ with geometric multiplicity of $\bar{r}$, each $\beta_i\in spec(\Omega)$ that satisfy $\beta_i(\beta_i+k)=\mu_i$ also has geometric multiplicity of $\bar{r}$.

Suppose the graph G does not contain directed spanning tree, then $\mu_i=0$ is not simple and it implies that $\beta_i=0$ is also not simple with similar algebraic and geometric multiplicity as have been shown in the above analyses. This completes the proof. □

The following *Theorem* provides the necessary and sufficient condition for the convergence of states $\tilde{\boldsymbol{x}}$ and $\tilde{\boldsymbol{v}}$.

Theorem 1. *Suppose graph F contains directed spanning tree and (13) governs the dynamics of $\tilde{\boldsymbol{x}}$ and $\tilde{\boldsymbol{v}}$. The states $\tilde{\boldsymbol{x}}$ and $\tilde{\boldsymbol{v}}$ converge asymptotically to $c1_N$ and 0_N respectively $\forall\tilde{\boldsymbol{x}}(t_0),\tilde{\boldsymbol{v}}(t_0)\in\mathbf{R}^N$ if and only if the sensing graph G contains directed spanning tree. Where c is a constant that depends on $\tilde{\boldsymbol{x}}(t_0)$ and $\tilde{\boldsymbol{v}}(t_0)$.*

Proof. ($\Rightarrow$) Let the system of interest be $\dot{p}(t) = \Omega p(t)$, $t > t_0$. Suppose that the graph G contains directed spanning tree, then from *Lemma 4*, Ω has an isolated zero eigenvalue. Also, the nonzero eigenvalues of Ω lie in the open left half plane. This means that the spectrum of Ω is similar to the spectrum of a *Laplacian* matrix where its associated graph contains directed spanning tree. With this spectrum of Ω, we can use the result from *Lemma 2*: the trajectories of the system satisfy $\lim_{t\to\infty} p(t) = (y^T p(t_0))q$ for any $p(t_0)$, where $\Omega q = 0$, $y^T\Omega = 0$ and $y^T q = 1$. From *Lemma 4* we know that $q = [1_N^T, 0_N^T]^T$, while y^T is the following: Let $[w_1^T, w_2^T]^T \in null(\Omega^T)$, then $-L^T w_2 = 0$ and $w_1 - kw_2 = 0$. This implies that if $w \in null(-L^T)$, then $[kw^T, w^T]^T \in null(\Omega^T)$. Thus, $y^T = [kw^T, w^T]$.

By replacing p by $[\tilde{\boldsymbol{x}}^T, \tilde{\boldsymbol{v}}^T]^T$, we obtain the following:

$$\lim_{t\to\infty}\begin{bmatrix}\tilde{\boldsymbol{x}}(t)\\ \tilde{\boldsymbol{v}}(t)\end{bmatrix} = \left(\begin{bmatrix}kw^T & w^T\end{bmatrix}\begin{bmatrix}\tilde{\boldsymbol{x}}(t_0)\\ \tilde{\boldsymbol{v}}(t_0)\end{bmatrix}\right)\begin{bmatrix}1_N\\ 0_N\end{bmatrix} = \begin{bmatrix}c1_N\\ 0_N\end{bmatrix}$$
$$\forall \tilde{\boldsymbol{x}}(t_0), \tilde{\boldsymbol{v}}(t_0) \in \mathbf{R}^N$$

where $c = k(w^T\tilde{\boldsymbol{x}}(t_0)) + w^T\tilde{\boldsymbol{v}}(t_0)$.

($\Leftarrow$) Suppose that the graph G does not contain directed spanning tree, then according to *Lemma 4*, the zero eigenvalue of Ω is not simple and it implies that there are more than one generalized eigenvectors correspond to the zero eigenvalue of Ω that will appear in the solution of the trajectories. Therefore, the states $\tilde{\boldsymbol{x}}$ and $\tilde{\boldsymbol{v}}$ will not converge asymptotically to $c1_N$ and 0_N, respectively, $\forall \tilde{\boldsymbol{x}}(t_0), \tilde{\boldsymbol{v}}(t_0) \in \mathbf{R}^N$. □

Remark 2. From *Theorem 1* we conclude that $\lim_{t\to\infty}\tilde{\boldsymbol{v}}(t) = 0_N$ and it implies that $\lim_{t\to\infty} v_i(t) = \gamma^*$. We also have that $\lim_{t\to\infty}\tilde{\boldsymbol{x}}(t) = c1_N = \tilde{\boldsymbol{x}}^f$ and it implies that $\lim_{t\to\infty}\boldsymbol{x}(t) = \tilde{\boldsymbol{x}}^f + (\lambda^*\boldsymbol{x}^d + \gamma^* 1_N t)$ and thus $\lim_{t\to\infty} x_i(t) = c + (\lambda^* x_i^d + \gamma^* t)$. These concludes that algorithms (4)-(6) solve the objectives (2)-(3) under fixed-directed sensing and communication graphs assuming the graphs contain directed spanning tree.

4 Formation Scaling under Switching Sensing and Communication Graphs

In this section, we consider that both sensing and communication graphs are switching due to unreliable communication channel and/or change in the environment. This means that a_{ij} and α_{ij} in (4)-(6) are now functions of time, i.e. $a_{ij}(t)$ and $\alpha_{ij}(t)$. We then write (12) as follows:

$$\begin{bmatrix}\dot{\tilde{\boldsymbol{x}}}(t)\\ \dot{\tilde{\boldsymbol{v}}}(t)\\ \dot{\tilde{\boldsymbol{\lambda}}}(t)\\ \dot{\tilde{\boldsymbol{\gamma}}}(t)\end{bmatrix} = \begin{bmatrix}\mathbf{0} & \mathbf{I} & \mathbf{0} & \mathbf{0}\\ -L_{\sigma(t)} & -k\mathbf{I} & \Gamma_{\sigma(t)} & k\mathbf{I}\\ \mathbf{0} & \mathbf{0} & -H_{\psi(t)} & \mathbf{0}\\ \mathbf{0} & \mathbf{0} & \mathbf{0} & -H_{\psi(t)}\end{bmatrix}\begin{bmatrix}\tilde{\boldsymbol{x}}(t)\\ \tilde{\boldsymbol{v}}(t)\\ \tilde{\boldsymbol{\lambda}}(t)\\ \tilde{\boldsymbol{\gamma}}(t)\end{bmatrix} \quad (16)$$

where σ and ψ are switching signals for sensing graph G and communication graph F respectively, i.e. $\sigma : [0,\infty) \to \mathcal{Z}$ and $\psi : [0,\infty) \to \bar{\mathcal{Z}}$ where $\mathcal{Z}$ and $\bar{\mathcal{Z}}$ are both finite index sets. Based on this settings, $L_{\sigma(t_i)}$ denotes matrix L at time t_i. For simplicity, we will write $G_{t_i} \in \bar{G}$ as the graph G at time t_i and its associated *Laplacian* matrix is L_{t_i}, where $\bar{G}$ denotes the set of all possible sensing graph. Henceforth, $F_{t_i} \in \bar{F}$ and H_{t_i} are defined analogously.

The following *Theorem* provides sufficient condition for the states $\tilde{\boldsymbol{\lambda}}$ and $\tilde{\boldsymbol{\gamma}}$ to converge to zeros under switching communication graph.

Lemma 5. Let $\lambda_N(t_0) = \lambda^*$ and $\gamma_N(t_0) = \gamma^*$. If the union of the communication graphs $\{F_{t_1}, F_{t_2}, ..., F_{t_m}\} \subset \bar{F}$ contain directed spanning tree, then $\lambda_i \to \lambda_N$ and $\gamma_i \to \gamma_N$ exponentially for all $i \in \mathbb{Z}^N$.

Proof. From (16), the dynamics of $\tilde{\boldsymbol{\lambda}}$ and $\tilde{\boldsymbol{\gamma}}$ are:

$$\dot{\tilde{\boldsymbol{\lambda}}}(t) = -H_{\psi(t)}\tilde{\boldsymbol{\lambda}}(t),$$
$$\dot{\tilde{\boldsymbol{\gamma}}}(t) = -H_{\psi(t)}\tilde{\boldsymbol{\gamma}}(t).$$

Referring to the work of [11], if the union of the communication graph contains directed spanning tree, then $\tilde{\lambda}$ and $\tilde{\gamma}$ reach consensus exponentially.

By noting that $\tilde{\boldsymbol{\lambda}}$ and $\tilde{\boldsymbol{\gamma}}$ have the same dynamics, we will first discuss $\tilde{\boldsymbol{\lambda}}$, and then the same conclusion can be applied to $\tilde{\boldsymbol{\gamma}}$. Since the union of the sensing graph contains directed spanning tree, from the work of [11], we know that $\tilde{\boldsymbol{\lambda}}$ reach consensus exponentially. Moreover, since $\lambda_N(t) = \lambda^*$ and $\gamma_N(t) = \gamma^*$ for all $t \geq 0$ which implies $\tilde{\lambda}_N(t) = 0$ and $\tilde{\gamma}_N(t) = 0$ for all $t \geq 0$, it can be concluded that $\tilde{\lambda}_i \to 0$ and $\tilde{\gamma}_i \to 0$ exponentially for all $i \in \mathbb{Z}^N$ which implies $\lambda_i \to \lambda_N$ and $\gamma_i \to \gamma_N$ exponentially for all $i \in \mathbb{Z}^N$. □

Based on *Lemma 5*, assuming that $\bigcup_{i=1}^{i=m} F_{t_i}$ contain directed spanning tree and the states $\tilde{\boldsymbol{\lambda}}$ and $\tilde{\boldsymbol{\gamma}}$ have already converged to zeros exponentially, then (16) can be reduced to:

$$\begin{bmatrix}\dot{\tilde{\boldsymbol{x}}}(t)\\ \dot{\tilde{\boldsymbol{v}}}(t)\end{bmatrix} = \begin{bmatrix}\mathbf{0} & \mathbf{I}\\ -L_t & -k\mathbf{I}\end{bmatrix}\begin{bmatrix}\tilde{\boldsymbol{x}}(t)\\ \tilde{\boldsymbol{v}}(t)\end{bmatrix} \quad (17)$$
$$= [\Omega_t]\begin{bmatrix}\tilde{\boldsymbol{x}}(t)\\ \tilde{\boldsymbol{v}}(t)\end{bmatrix}; t > t_0$$

The following *Theorem* provides the sufficient condition for the convergence of $\tilde{x}$ and $\tilde{v}$:

Theorem 2. *Consider the dynamics (17). If the union of the sensing graphs $\{G_{t_1}, G_{t_2}, ..., G_{t_m}\} \subset \bar{G}$ contain directed spanning tree, then $\lim_{t\to\infty}\tilde{\boldsymbol{x}}(t) = c1_N$ and $\lim_{t\to\infty}\tilde{\boldsymbol{v}}(t) = 0_N$, $\forall t > t_0$.*

Proof. For simplicity, let $\boldsymbol{p} = [\tilde{\boldsymbol{x}}, \tilde{\boldsymbol{v}}]^T$, so (17) can be written as $\dot{\boldsymbol{p}}(t) = \Omega_t \boldsymbol{p}(t)$. From *Lemma 4*, we know that the spectral properties of Ω is related to $-L$. That is, zero is an eigenvalue of Ω and the nonzero eigenvalues of Ω lies on the open left-half plane, and the zero eigenvalue of Ω is isolated when the graph G contains directed spanning tree. We will show that by some transformation matrix, Ω can be transformed into a matrix with similar structure to $-L$ (nonpositive diagonals, nonnegative off-diagonals, and zero row-sum).

Consider the transformation coordinate $\hat{\boldsymbol{p}} = T\boldsymbol{p}$ with:

$$T = \begin{bmatrix} \mathbf{I} & \mathbf{I} \\ \mathbf{I} & \mathbf{0} \end{bmatrix}, \; T^{-1} = \begin{bmatrix} \mathbf{0} & \mathbf{I} \\ \mathbf{I} & -\mathbf{I} \end{bmatrix}$$

Thus, $\dot{\hat{\boldsymbol{p}}}(t) = T\Omega_t T^{-1}\hat{\boldsymbol{p}}(t) = \hat{\Omega}_t\hat{\boldsymbol{p}}(t)$, where:

$$\hat{\Omega}_t = \begin{bmatrix} -(k-1)\mathbf{I} & (k-1)\mathbf{I} - L_t \\ \mathbf{I} & -\mathbf{I} \end{bmatrix}.$$

By choosing k appropriately, i.e. it satisfies

$$k \geq max_i\{l_{ii_t}\} + 1, \forall t$$

where l_{ii_t} is the diagonal entry of L_t, $-\hat{\Omega}_t$ has a similar structure to a *Laplacian* matrix. Furthermore, since the coordinate transformation does not change the eigenvalues of, *Lemma 4* is applicable to $\hat{\Omega}_t$.

From *Theorem 2*, we expect that $\lim_{t\to\infty}\tilde{\boldsymbol{x}}(t) = c1_N$ and $\lim_{t\to\infty}\tilde{\boldsymbol{v}}(t) = 0_N$. In this case, we expect that $\lim_{t\to\infty}\boldsymbol{p}(t) = [c1_N^T, 0_N^T]$. It implies that:

$$\begin{aligned} \lim_{t\to\infty}\hat{\boldsymbol{p}}(t) &= \lim_{t\to\infty} T\boldsymbol{p}(t) = T\lim_{t\to\infty}\boldsymbol{p}(t) \\ &= \begin{bmatrix} \mathbf{I} & \mathbf{I} \\ \mathbf{I} & \mathbf{0} \end{bmatrix}\begin{bmatrix} c1_N \\ 0_N \end{bmatrix} = \begin{bmatrix} c1_N \\ c1_N \end{bmatrix} \end{aligned}$$

From the above result, we can see that $\lim_{t\to\infty}\tilde{\boldsymbol{x}}(t) = c1_N$ and $\lim_{t\to\infty}\tilde{\boldsymbol{v}}(t) = 0_N$ if and only if the system $\dot{\hat{\boldsymbol{p}}}(t) = \hat{\Omega}_t\hat{\boldsymbol{p}}(t)$ reaches consensus. Moreover, since $-\hat{\Omega}_t$ has a similar structure to a *Laplacian* matrix, the problem $\dot{\hat{\boldsymbol{p}}}(t) = \hat{\Omega}_t\hat{\boldsymbol{p}}(t)$ is a regular consensus problem under switching graph where we can use the results of [15].

Matrix $\hat{\Omega}_t$ can be decomposed into: $\hat{\Omega}_t = -(\mathcal{D}_t - \mathcal{A}_t)$, where:

$$\mathcal{D}_t = \begin{bmatrix} (k-1)\mathbf{I} & \mathbf{0} \\ \mathbf{0} & \mathbf{I} \end{bmatrix}; \mathcal{A}_t = \begin{bmatrix} \mathbf{0} & (k-1)\mathbf{I} - L_t \\ \mathbf{I} & \mathbf{0} \end{bmatrix}$$

Let S_t be the graph associated with $\hat{\Omega}_t$, and $\mathcal{A}_t$ is the adjacency matrix extracted from S_t, and its entry is nonnegative with the proper choice of δ. The idea is to show that S_t contains directed spanning tree if and only if G_t contains directed spanning tree.

Since the coordinate transformation does not change the eigenvalues, then $spec(\Omega_t) = spec(\hat{\Omega}_t)$. From *Lemma 4*, when G_t contains directed spanning tree, then 0 is an isolated eigenvalue of Ω_t and the nonzero eigenvalues of Ω_t lies on the open left-half plane. Since $spec(\Omega_t) = spec(\hat{\Omega}_t)$, then it implies that 0 is an isolated eigenvalue of $\hat{\Omega}_t$ and the nonzero eigenvalues of $\hat{\Omega}_t$ lies on the open left-half plane. Due to *Lemma 1*, this implies that S_t contains directed spanning tree. So, these show that G_t contains directed spanning tree implies that contains directed spanning tree. The reverse is also true since *Lemma 4* and *Lemma 1* show the necessary and sufficient conditions of spectral properties of Ω_t and the Laplacian matrix. These show that S_t contains directed spanning tree if and only if G_t contains directed spanning tree.

Since S_t contains directed spanning tree if and only if G_t contains directed spanning tree, then we can also conclude that: if the union of the sensing graphs $\bigcup_{i=1}^{i=m} G_{t_i}$ contain directed spanning tree, then the union of S_t, $\bigcup_{i=1}^{i=m} S_{t_i}$ also contains directed spanning tree.

Based on the above reasoning, we can apply the result from [15] to the system $\dot{\hat{\boldsymbol{p}}}(t) = \hat{\Omega}_t\hat{\boldsymbol{p}}(t)$. That is, when $\bigcup_{i=1}^{i=m} G_{t_i}$ contain directed spanning tree, then $\hat{p}$ reaches consensus which implies that $\lim_{t\to\infty}\tilde{\boldsymbol{x}}(t) = c1_N$ and $\lim_{t\to\infty}\tilde{\boldsymbol{v}}(t) = 0_N$. □

Since $\lim_{t\to\infty}\tilde{\boldsymbol{x}}(t) = c1_N$ and $\lim_{t\to\infty}\tilde{\boldsymbol{v}}(t) = 0_N$, we can use the same reasoning from Remark 2 where we conclude that the objectives (2) and (3) are solved under switching graph topology.

5 Numerical Examples

In this section, simulation example of two dimensional problem of three agents to produce formation with adjustable scaling factor and adjustable group's velocity under fixed directed graph and switching-directed graph will be presented. The MATLAB code for the simulation can be accessed in the following URL: github formation tracking.

5.1 Fixed Graph

We consider 5 agents which will be tasked to form a pentagon. The communication graph and sensing graph are shown in Figure 2. The sensing graph has no leader while the communication graph denotes agent 5 as the leader. In the fixed graph case, all nonzero adjacency entries are set to one.

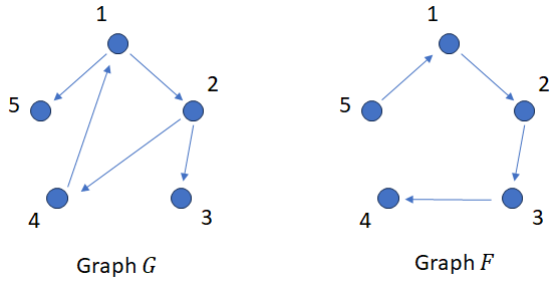

Figure 2: Sensing graph and communication graph: fixed graph case.

The simulation is done in two dimensional problem, where $x_i = [x_i^1, x_i^2]^T \in \mathbb{R}^2$. The desired formation pattern for each agent is the following:

$$x_i^d = 5\begin{bmatrix} \cos\left((0.1 + (i-1)0.4)\,\pi\right) \\ \sin\left((0.1 + (i-1)0.4)\,\pi\right) \end{bmatrix}, \; i = 1, 2, 3, 4, 5.$$

which will form a pentagon. Initially, agents will form the formation with scaling factor equals one with desired group velocity equals zero. Then, agents will be tasked to move in the x^1 axis and change the formation scaling factor to 0.25, then after some time agents will move in the x^2 axis and increase their formation scaling factor from 0.25 to 0.5.

The initial conditions of agent 5 to achieve these taks are as follow: $\lambda_5(t_0^1) = \begin{bmatrix}1\\1\end{bmatrix}$, $\lambda_5(t_0^2) = \begin{bmatrix}0.25\\0.25\end{bmatrix}$, $\lambda_5(t_0^3) = \begin{bmatrix}0.5\\0.5\end{bmatrix}$, $\gamma_5(t_0^1) = \begin{bmatrix}0\\0\end{bmatrix}$, $\gamma_5(t_0^2) = \begin{bmatrix}0.75\\0\end{bmatrix}$, and $\gamma_5(t_0^3) = \begin{bmatrix}0\\0.75\end{bmatrix}$. Meanwhile, the initial conditions for the remaining states are random number. Agents' movement in 2 dimensional plane are shown in Figure 3. Meanwhile, the evolution of agents' velocities are depicted in Figures 4 and 5. In Figure 3, $\circ$ shows the initial positions, $*$ shows the formation with scaling factor of 1, $\square$ shows the formation with scaling factor of 0.25, and $\triangle$ shows the formation with scaling factor of 0.5.

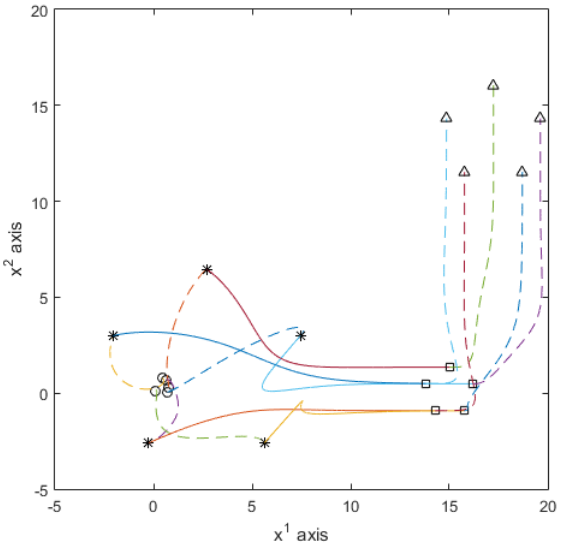

Figure 3: Agent's movement in 2 dimensional plane: fixed graph case.

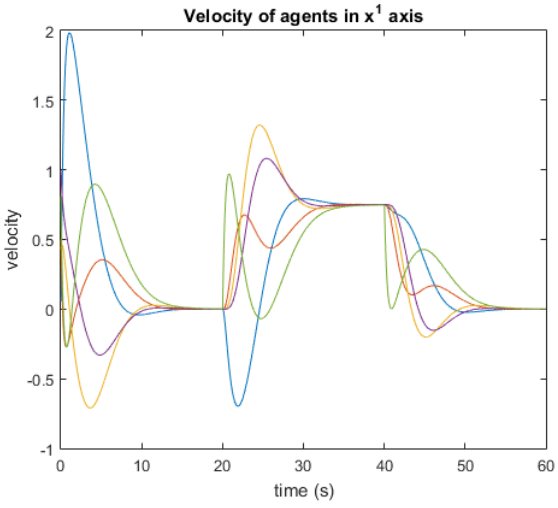

Figure 4: Agent's velocities in x^1 axis.

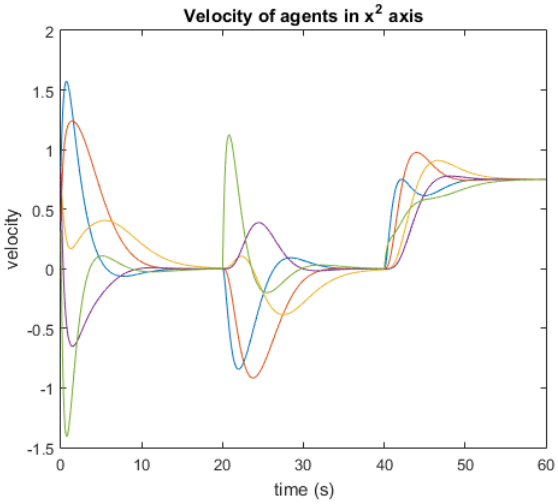

Figure 5: Agent's velocities in x^2 axis.

5.2 Switching Graph

The sensing graph and communication graph used in the simulation are shown in Figures 6 and 7. In the switching case, we vary the adjacency weight as shown in the figures. Note that each G_1 and G_2 also F_1 and F_2 does not contain a spanning tree, but their union contains a spanning tree. The sensing graph G and communication graph F are assumed to be switching from G_1 to G_2, F_1 to F_2, and vice versa respectively. Each of the $G_i, F_i; i = 1, 2$ is set to be active for 1.25 seconds before it switches. Following are the desired formation pattern: $x^{1d} = [1 \quad 2 \quad 3]^T$, $x^{2d} = [1 \quad \sqrt{3} \quad 1]^T$. Where each x^{1d} and x^{2d} refers to the desired formation pattern in each axis. The first objective is to achieve a formation pattern with a scaling factor of 1 and desired velocity of 0; while the second objective is to achieve a formation pattern with a scaling factor of 0.25 and desired velocity of $v^{1*} = 0.05$ and $v^{2*} = 0.025$.

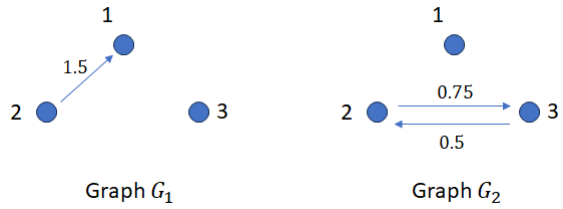

Figure 6: Sensing graphs: switching graph case.

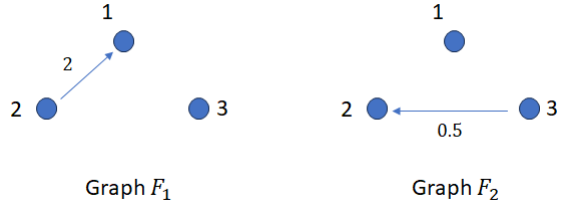

Figure 7: Communication graphs: switching graph case.

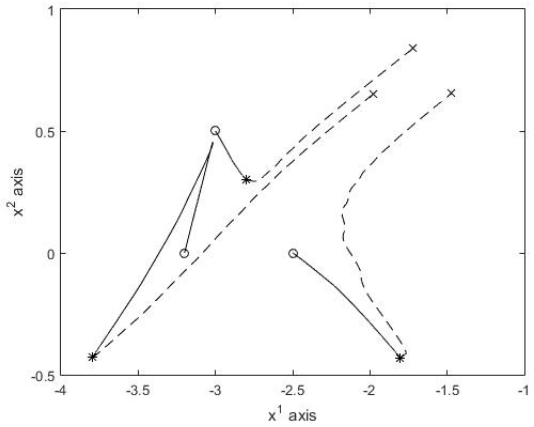

Figure 8: Agents' movement in 2 dimensional plane.

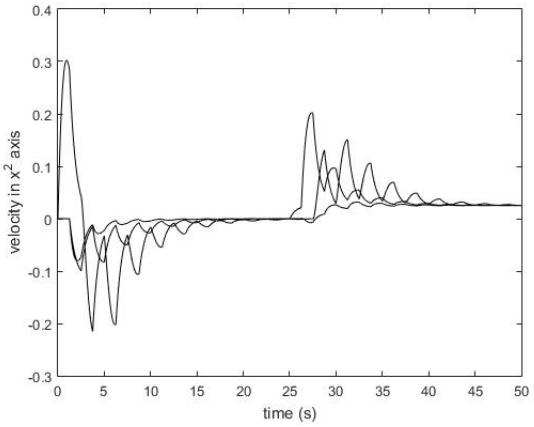

Figure 10: Evolution of Agents' velocity in $\boldsymbol{x^2}$ axis.

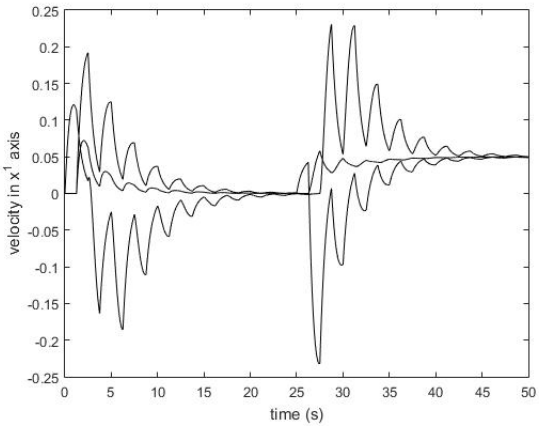

Figure 9: Evolution of Agents' velocity in $\boldsymbol{x^1}$ axis.

In Figure 8, o shows the initial positions of agents, * shows the positions representing the first objective and x shows the positions representing the second objetive. The solid line represents the trajectories during the first objective, while the dashed line represents the trajectories during the second objective. Meanwhile, the evolution of agents' velocities are shown in Figure 9 and 10. We can see that there are ripples in the velocity response compared to the fixed graph case. This happens due to the switching graph setting.

6 Conclusion

In this paper, the problem of scalable distributed formation of double integrator agents where the leader agent determines the scaling factor of the formation as well as the velocity of the entire agents has been presented. It is shown that under switching sensing and communication graphs, the desired scaled formation and group's velocity are achieved if the union of the sensing and communication graphs contains a spanning tree. The results are verified with a simulation example of three agents achieving adjustable formation scaling factor and group's velocity.

Acknowledgement: The Authors would like to thank the Indonesian National Research and Innovation Agency, especially the Research Organization for Aeronautics and Space with research grant number 16/III.1/HK/2023, for the support throughout this research.

References

[1] Azam, M. A., Mittelmann, H. D., and Ragi, S. Uav formation shape control via decentralized markov decision processes. *Algorithms 14*, 3 (2021), 91.

[2] Coogan, S., and Arcak, M. Scaling the size of a formation using relative position feedback. *Automatica 48*, 10 (2012), 2677–2685.

[3] Coogan, S., Arcak, M., and Egerstedt, M. Scaling the size of a multiagent formation via distributed feedback. In *Proceedings of 50th Conference on Decision and Control* (2011), IEEE, pp. 994–999.

[4] Djamari, D. W. Scalable formation of heterogeneous agents considering unknown disturbances. *Asian J. of Control 23*, 4 (2021), 1631–1642.

[5] Djamari, D. W. Distributed position estimation approach for multiagent formation with size scaling. *Asian J. of Control 24*, 1 (2022), 439–447.

[6] Hu, Z., and Yang, J. Distributed optimal formation algorithm for multi-satellites system with time-varying performance function. *International Journal of Control 93*, 5 (2020), 1015–1026.

[7] Lin, Z., Francis, B., and Maggiore, M. Necessary and sufficient graphical conditions for formation control of unicycles. *IEEE Trans. Automatic Control 50*, 1 (2005), 121–127.

[8] Lin, Z., Wang, Z., Fue, M., and Han, Z. Necessary and sufficient graphical conditions for affine formation control. *IEEE Trans. Automatic Control 61*, 10 (2016), 2877–2891.

[9] Massioni, P., Keviczky, T., Gill, E., and Verhaegen, M. A decomposition-based approach to linear time-periodic distributed control of satellite formations. *IEEE Transactions on Control Systems Technology 19*, 3 (2011), 481–492.

[10] Mesbahi, M., and Egerstedt, M. *Graph Theoretic Methods in Multiagent Networks*. Princeton Series in Applied Mathematics, 2010.

[11] Moreau, L. Stability of continuous-time distributed consensus algorithms. In *2004 43rd IEEE conference on decision and control (CDC)(IEEE Cat. No. 04CH37601)* (2004), vol. 4, IEEE, pp. 3998–4003.

[12] Naethe, P., Asgari, M., Kneer, C., Knieps, M., Jenal, A., Weber, I., Moelter, T., Dzunic, F., Deffert, P., Rommel, E., Delaney, M., Baschek, B., Rock, G., Bongartz, J., and Burkart, A. Calibration and validation from ground to airborne and satellite level: Joint application of time-synchronous field spectroscopy, drone, aircraft and sentinel-2 imaging. *PFG - Journal of Photogrammetry, Remote Sensing and Geoinformation Science 91*, 1 (2023), 43–58.

[13] Oh, K.-K., Park, M.-C., and Ahn, H.-S. A survey of multi-agent formation control. *Automatica 53* (2015), 424–440.

[14] Ong, C. J., Djamari, D. W., and Hou, B. A governor approach for consensus of heterogeneous systems with constraints under a switching network. *Automatica 122*, - (2020), 109239.

[15] Ren, W. Consensus seeking in multiagent systems under dynamically changing interaction topologies. *IEEE Trans. Automatic Control 50*, 5 (2005), 655–661.

[16] Ren, W. Consensus strategies for cooperative control of vehicle formations. *IET Control Theory & Applications 1*, 2 (2007), 505–512.

[17] Schanbusch, R., Kristiansen, R., and Nicklasson, P. Spacecraft formation reconfiguration with collision avoidance. *Automatica 47*, 7 (2011), 1443–1449.

[18] Sun, Y., Ma, G., Liu, M., and Chen, L. Distributed finite-time configuration containment control for satellite formation. *Proceedings of the Institution of Mechanical Engineers, Part G: Journal of Aerospace Engineering 231*, 9 (2017), 1609–1620.

[19] Tran, D., Yucelen, T., and Pasiliao, E. Multiplex information networks for spatially evolving multiagent formations. In *Proceedings of the American Control Conference* (Boston, MA, USA, 2016), pp. 1912–1917.

[20] Wang, C., Xie, G., and Cao, M. Forming circle formations of anonymous mobile agents with order preservation. *IEEE Trans. Automatic Control 58*, 12 (2013), 3248–3254.

[21] Wang, Y., Chen, X., Ran, D., Zhao, Y., Chen, Y., and Bai, Y. Spacecraft formation reconfiguration with multi-obstacle avoidance under navigation and control uncertainties using adaptive artificial potential function method. *Astrodynamics 4*, 1 (2020), 41–56.

[22] Zheng, Z., Qian, M., Li, P., and Yi, H. Distributed adaptive control for uav formation with input saturation and actuator fault. *IEEE Access 7*, - (2019), 144638 – 144647.